ACES Asian Chemical Editorial Society

DOI: 10.1002/ajoc.201600100

ASIAN JOURNAL OF ORGANIC CHEMISTRY
Full Paper

Solar Cell Sensitizers

Metal-Free Indeno[2,1-*b*]thiophene-Based Sensitizers for Dye-Sensitized Solar Cells

Chia-Jung Liang,[a] Yu-Ju Lin,[a, b] Yung-Sheng Yen,[a, c] Jiann T. Lin,*[a] and Ming-Chang P. Yeh*[b]

Abstract: A series of indeno[2,1-*b*]thiophene-containing organic dyes (**IDT1**–**IDT5**) have been synthesized, and their UV/Vis spectra extend beyond 700 nm. These dyes were employed as sensitizers for dye-sensitized solar cells (DSSCs). Among them, dyes **IDT3**–**IDT5** with a thiophene unit conjugated with an anchor have better light harvesting ability and higher J_{SC} values. Dye aggregation contributes substantially to the photocurrent in the near infrared region. The dye **IDT5**, with chenodeoxycholic acid (CDCA) as the co-adsorbent, has the highest power conversion efficiency (5.06%) under AM 1.5G simulated sunlight irradiation, which is 68% of the standard device based on N719 dye.

Introduction

Being cost effective and simple in device fabrication, dye-sensitized solar cells (DSSCs) have attracted considerable interest since O'Regan and Grätzel's seminal work, and the cell performance continues to improve.[1] Ruthenium complexes are probably the most reliable sensitizers so far owing to the high cell efficiency and long term stability.[2] However, the natural reserves of ruthenium are limited. Therefore, many researchers have turned their attention to zinc-porphyrins[3] and metal-free organic dyes,[4] and cells based on these dyes, with efficiencies surpassing that of ruthenium dyes, have been achieved. Metal-free organic dyes have several advantages: easy synthesis and purification, and high molar extinction coefficients. Up to now, the best cell efficiency under AM 1.5G simulated sunlight irradiation has reached 13.0%[5] and 14.0%[6] for single dye and co-dye systems, respectively. Organic sensitizers usually consist of a D–π–A segment (D, a π-electron-rich donor; π, a conjugated spacer; A, a π-electron-deficient acceptor).

Rigidified π-spacers are interesting because the planarity and rigidity of the segment may help with reducing re-organization energy and benefit electronic communication between the donor and the acceptor, leading to better light harvesting.[7] Many rigidified spacers of symmetrical structure such as indenofluorene,[8] tetrathienoacene (TTA),[9] indaceno[1,2-*b*:5,6-*b*′]dithiophene,[10] anthracene,[11] phenothiazine,[12] 4*H*-dithieno[3,2-*b*:2′,3′-*d*]pyrrole (DTP),[13] and dithieno[3,2-*f*:2′,3′-*h*]quinoxaline (DTQ)[14] have been used for the construction of the sensitizers. There are rare examples of rigidified spacers with an asymmetric structure.[15] Blanchard and Roncali reported an indeno[2,1-*b*]thiophene (IDT) derivative with an triarylamine substituent and a dicyanovinyl substituent at the 2 and 8 positions of IDT, respectively. The compound has an intramolecular charge transfer (ICT) absorption maximum at 610 nm and an absorption onset point at ~750 nm, indicating that the ICT entity is a good π-linker. In view of the fact that dibenzofulvene has been successfully used as the π-linker in dipolar dyes,[16] we decided to adopt IDT as the π-linker with an arylamine donor and 2-cyanoacrylic acid acceptor (also as the anchor) connected to the 2 and 8 positions of IDT, respectively. We also introduced a thiophene unit between the IDT and the anchor. Physical properties, theoretical computation, and the DSSC performance of the dyes will be also discussed. While this work was being completed, we were aware that Roncali reported a dye based on 2,8-disubstituted IDT with a power conversion efficiency of 2.00% (J_{SC} = 4.70 mA cm^2, V_{OC} = 564 mV, fill factor (FF) = 0.72).[17]

Results and Discussion

Synthesis of Sensitizers

The organic dyes, **IDT1**–**IDT5**, are shown in Figure 1. Bromination of 8*H*-indeno[2,1-*b*]thiophen-8-one (**1**) gave 2-bromo-8*H*-indeno[2,1-*b*]thiophen-8-one (**2**).[18] Condensation reaction of **2** with ethyl cyanoacetate afforded **3**.[19] The **IDT1** and **IDT2** dyes

[a] Dr. C.-J. Liang, Y.-J. Lin, Dr. Y.-S. Yen, Prof. Dr. J. T. Lin
Institute of Chemistry
Academia Sinica
Taipei, 115 (Taiwan)
E-mail: jtlin@gate.sinica.edu.tw

[b] Y.-J. Lin, Prof. Dr. M.-C. P. Yeh
Department of Chemistry
National Taiwan Normal University
Taipei, 117 (Taiwan)
E-mail: cheyeh@ntnu.edu.tw

[c] Dr. Y.-S. Yen
Assistant Research Scholar of the National
Science Council of ROC (Taiwan)

Supporting information for this article can be found under http://dx.doi.org/10.1002/ajoc.201600100.

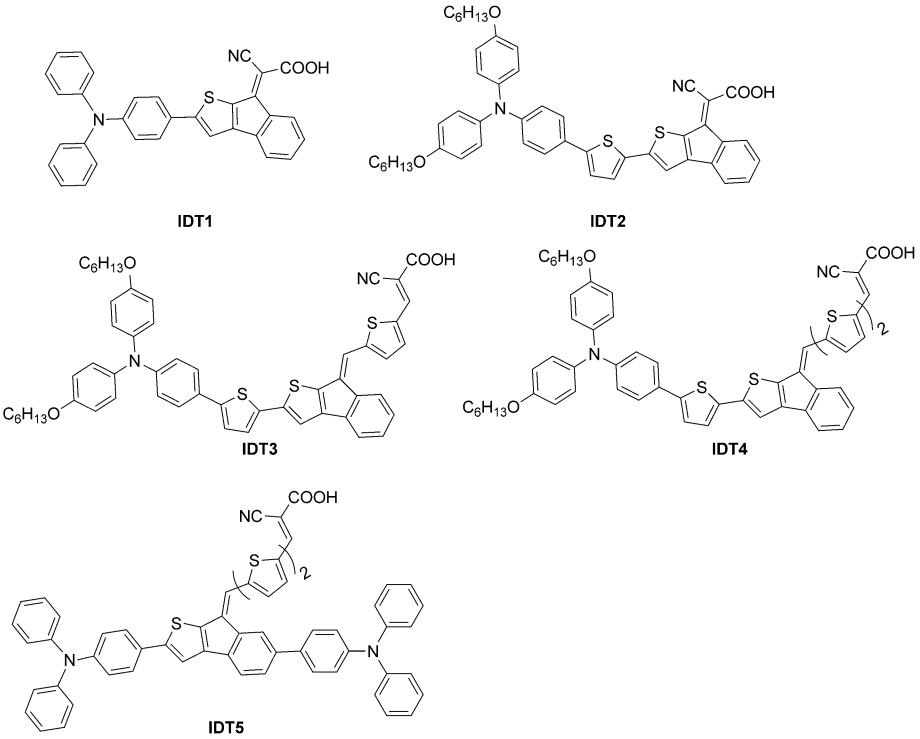

Figure 1. The structures of the dyes.

were synthesized by Stille cross-coupling reactions of compound **3** with *N*,*N*-diphenyl-4-(tributylstannyl)aniline and 4-(hexyloxy)-*N*-(4-(hexyloxy)-phenyl)-*N*-(4-(5-(tributylstannyl)thiophen-2-yl)phenyl)aniline, respectively, followed by a hydrolysis reaction (Scheme 1). Stille cross-coupling reaction of **2** with 4-(hexyloxy)-*N*-(4-(hexyloxy)-phenyl)-*N*-(4-(5-(tributylstannyl)thiophen-2-yl)phen-yl)aniline, using $PdCl_2(PPh_3)_2$ as the catalyst precursor, provided **6**. Treatment of **6** with borane-*tert*-butylamine and aluminum chloride afforded **7**. Subsequent condensation reaction with **7** and thiophene-2,5-dicarbaldehyde under ultrasonic conditions generated **8**, which underwent Knoevenagel condensation with cyanoacetic acid in the presence of ammonium acetate to give the desired product **IDT3**. Compound **IDT4** was prepared similarly to **IDT3** except that **7** was treated with 2,2′-bithiophenyl-5,5′-dicarbaldehyde instead of thiophene-2,5-dicarbaldehyde. To synthesize **IDT5**, with two donors, we started from 6-bromo-8*H*-indeno[2,1-*b*]thiophen-8-one (**10**) and followed the same procedures as described for **IDT4**.

UV/Vis Absorption Properties

The UV/Vis absorption spectra and the corresponding data of the IDT dyes in THF (dye concentration: 10 μm) are depicted in Figure 2 and Table 1, respectively. The longest wavelength is ascribed to the intramolecular charge transfer (ICT) band from donor to acceptor, and the shorter wavelength absorption bands are attributed to the aromatic rings π–π* transition. The onset of the ICT band is >650 nm for all the compounds. The optical HOMO/LUMO gap, E_{0-0}, derived from the intersection

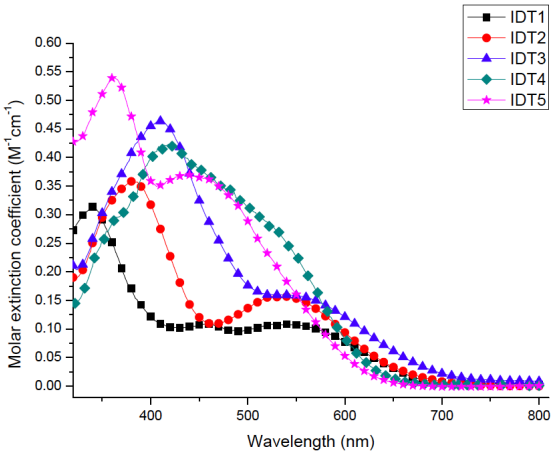

Figure 2. UV/Vis absorption spectra of the dyes in THF (10 μM).

of the absorption and emission (see below) of the ICT band, is also included in Table 1 for each dye. The ICT band of **IDT1** has the largest E_{0-0} value among all the compounds because of the shortest conjugation length of **IDT1**. Elongation of the conjugation length by insertion of a thiophene entity between the triarylamine and the IDT entities (**IDT2**) results in a redshift (i.e., smaller E_{0-0} value) of the ICT band. Enhancement of the electron-donating power of the triarylamine entity by adding alkoxy substituents is certainly also beneficial to the smaller E_{0-0} value. Extending the conjugation length by insertion of thienyl entities between the 2-cyanoacrylic acid anchor and the IDT entity (**IDT3** and **IDT4**) further decreases the E_{0-0} value

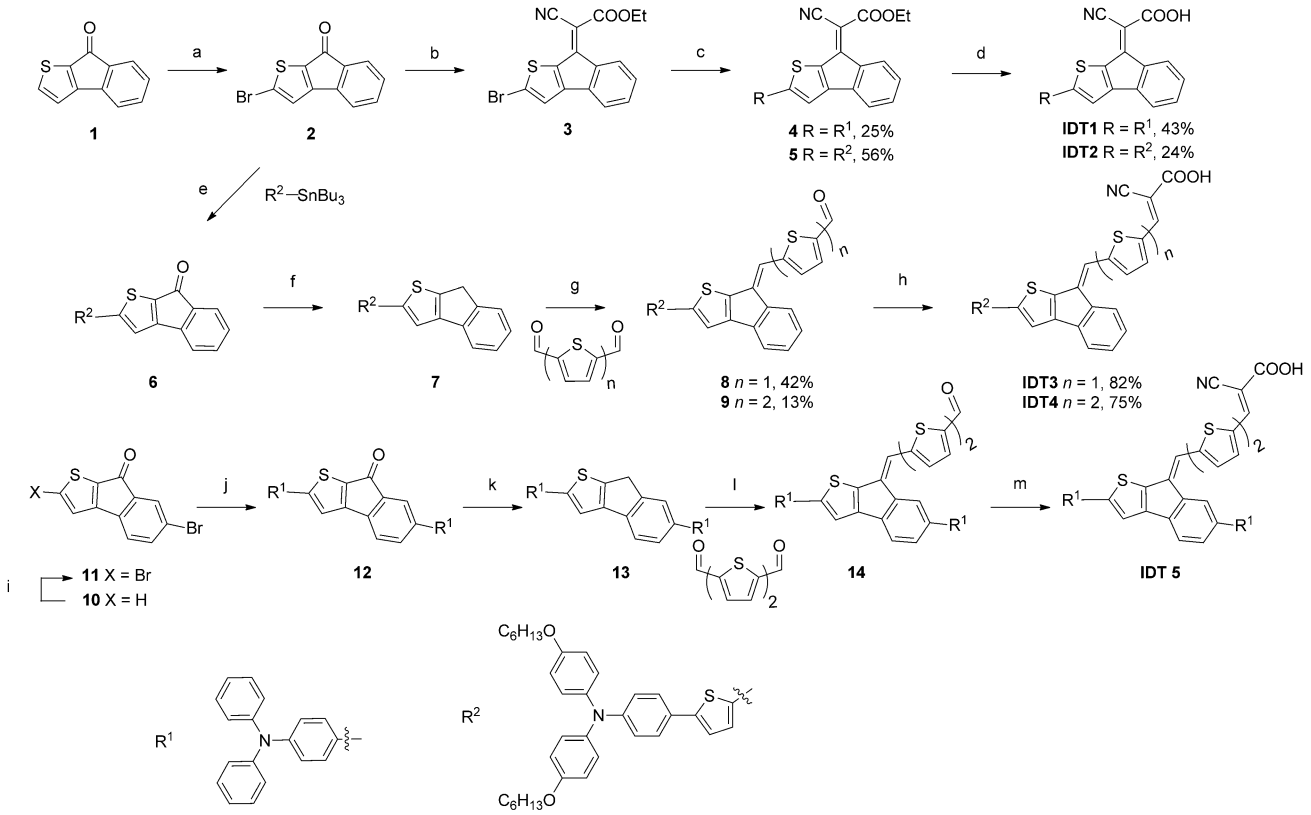

Scheme 1. Synthetic routes for the preparation of the dyes **IDT1**–**IDT5**. a) Br_2, $NaHCO_3$, $CHCl_3$, 8 h, 86%; b) ethyl cyanoacetate, *N*-methylmorpholine, $TiCl_4$, CH_2Cl_2, 2 h, 62%; c) *N*,*N*-diphenyl-4-(tributylstannyl)aniline, $Pd(PPh_3)_4$, PPh_3, toluene, 110 °C, 1 d; d) 2 M $LiOH_{(aq)}$, THF, 12 h; e) $PdCl_2(PPh_3)_2$, DMF, 80 °C, 14 h, 97%; f) $AlCl_3$, BH_3tBuNH_2, CH_2Cl_2, 4 h, 58%; g) KO*t*Bu, THF, MeOH, ultrasonic irradiation, 3 h; h) cyanoacetic acid, ammonium acetate, acetic acid, 105 °C, 12 h; i) $NaHCO_3$, $CHCl_3$, Br_2, 12 h, 64%; j) *N*,*N*-diphenyl-4-(tributylstannyl)aniline, $Pd(PPh_3)_4$, PPh_3, DMF, 80 °C, 1 d; k) $AlCl_3$, BH_3tBuNH_2, CH_2Cl_2, 4 h, 46%; l) KO*t*Bu, THF, MeOH, ultrasonic irradiation, 3 h, 37%; m) cyanoacetic acid, ammonium acetate, acetic acid, 105 °C, 12 h, 82%.

Table 1. Electro and optical parameters of the dyes.

Dye	λ_{abs} [nm] ($\varepsilon \times 10^{-4}$ [$M^{-1}cm^{-1}$])[a]	λ_{em} [nm][a]	λ_{abs} (TiO_2) [nm][b]	E_{gap}^{opt} [eV][c]	$E_{1/2}$ (ox) (E_p) [mV][d]	E[ox] [V vs. NHE]	E_{0-0}* [V vs. NHE][e]	HOMO/LUMO [eV]
IDT1	340 (3.14), 540 (1.08)	645	551	2.06	544 (123)	1.24	−0.82	5.64/3.58
IDT2	382 (3.60), 536 (1.57)	656	572	2.03	260 (114)	0.96	−1.07	5.36/3.33
IDT3	410 (4.64), 546 (1.59)	693	560	1.93	244 (119), 483 (156)	0.94	−0.99	5.34/3.41
IDT4	419 (4.24), 530 (2.69)	710	582	2.00	243 (137)	0.94	−1.06	5.34/3.34
IDT5	363 (5.40), 437 (3.70)	673	457	2.00	372 (158), 563 (248)	1.07	−1.10	5.47/3.30

[a] Recorded in THF at 298 K. [b] Recorded in the TiO_2 films. [c] The bandgap, E_{0-0}, was derived from the intersection of the absorption and emission spectra. [d] Recorded in THF. $E_{ox} = 1/2(E_{pa} + E_{pc})$, $\Delta E_p = E_{pa} - E_{pc}$ where E_{pa} and E_{pc} are the peak anodic and cathodic potentials, respectively. The oxidation potential reported is adjusted to the potential of ferrocene, which was used as an internal reference. The values in parentheses are the peak separation of cathodic and anodic waves. i: irreversible. Scan rate: 100 mV s^{-1}. [e] Excited-state potential.

of the ICT band. Dye **IDT3** has a smaller E_{0-0} value than **IDT4** despite the fact that the latter has a longer conjugated spacer. Clearly, the longer conjugated spacer weakens the electronic communication between the donor and the acceptor in **IDT4**. Although **IDT5** has an extra triarylamine donor at the IDT entity compared with the other dyes, the former does not have the smallest E_{0-0} value. Possibly the large twist angle (33.87°, see below) between IDT and the arylamine moiety at the phenyl ring of IDT renders inefficient electronic communication between the extra donor and the acceptor. The extra two thiophene entities in **IDT5** likely also weaken the electronic communication between the donors and the acceptor.

Compared with the solution spectrum, dyes adsorbed on the TiO_2 form *J*-aggregates based on the following observations: (1) the film spectrum of the dyes adsorbed on TiO_2 is broader, with an onset at >700 nm; (2) the film absorption spectrum becomes narrower at the longer wavelength side upon addition of chenodeoxycholic acid (CDCA) co-adsorbent, except for **IDT3** and **IDT4** (Figure 3). Nonetheless, the λ_{abs} value of the ICT band (from the deconvoluted absorption) is

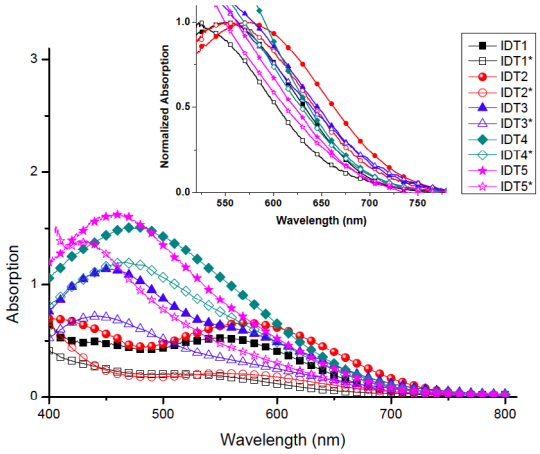

Figure 3. Absorption spectra of the IDT dyes in TiO_2 films with (marked with *) or without 30 mM CDCA. Inset: Expansion of the spectra in the 500–775 nm range.

blueshifted for **IDT3** and **IDT4**, indicating the existence of dye aggregation. The dyes are weakly emissive and the emission wavelength decreases in the order **IDT4** > **IDT3** > **IDT5** > **IDT2** > **IDT1**, which is in line with the absorption spectra except for **IDT5**. Possibly **IDT5** has a more planar structure in the excited state.

Electrochemical Properties

Cyclic voltammetry (CV) and differential pulse voltammetry (DPV) methods were used for measuring the electrochemical properties of **IDT1**–**IDT5** in THF at the concentration of 1 mM with ferrocene as the internal standard (Figure 4). The relevant

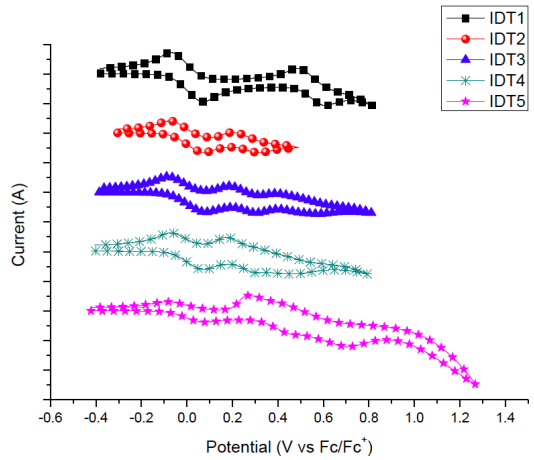

Figure 4. Cyclic voltammograms of the IDT dyes.

data from the CV measurements are listed in Table 1. Quasi-reversible redox waves were recorded for **IDT1**–**IDT4**, which are attributed to oxidation of the arylamine donor. There exist irreversible redox waves at more anodic potentials for **IDT3** and **IDT4**, which are attributed to the oxidation of oligothiophene. These waves are easier to recognize in the DPV plots. Dyes **IDT3** and **IDT4** have comparable oxidation potentials, although the latter has an extra thiophene ring. This outcome can be attributed to the minimal contribution of the thiophene ring next to the acceptor to the HOMO orbital (Figure S1 in the Supporting Information). The highest occupied molecular orbital (HOMO) energy levels were calculated from the first oxidation potential (ferrocene = 5.1 eV). The LUMO energy levels are derived from the equation $E_{LUMO} = E_{HOMO} - E_{0-0}$ in which the zero–zero band gap (E_{0-0}) values were obtained from the intersection of the normalized absorption and emission spectra. The excited-state potentials (E_{0-0}*) of **IDT1**–**IDT5** were calculated from the first oxidation potential and E_{0-0}. The values range from −0.82 to −1.10 V versus the normal hydrogen electrode (NHE), indicating that there is sufficient thermodynamic driving force for charge injection to the conduction band of TiO_2 (−0.5 V vs. NHE). On the other hand, the first oxidation potentials (0.94–1.24 V) are more positive than the redox potential of the I^-/I_3^- electrolyte (0.4 V vs. NHE), suggesting that regeneration of the oxidized dye is thermodynamically favorable.

Photovoltaic Devices

The DSSCs were fabricated with 0.16 cm^2 nanocrystalline anatase TiO_2 and were soaked in a THF solution of the sensitizer (10^{-4} M) for 12 h. The electrolyte was composed of 0.5 M LiI, 0.05 M I_2, and 0.5 M *tert*-butylpyridine in acetonitrile. The photocurrent density–photovoltage (*J*–*V*) curves under simulated AM 1.5G sunlight are depicted in Figure 5. The corresponding cell

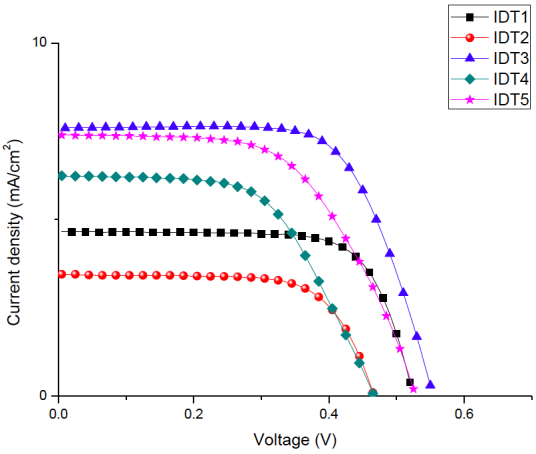

Figure 5. *J*–*V* curves of DSSCs based on the **IDT1**–**IDT5** dyes.

performance data are shown in Table 2. The incident photocurrent conversion efficiencies (IPCE) of the dyes are presented in Figure 6. Although the IPCE spectra are fairly broad, extending to > 700 nm, the efficiencies in the whole absorption range are all < 60% and the best photocurrent (J_{SC}) and photovoltage (V_{OC}) values are below 8 mA cm^2 and 0.570 V, respectively. Significant dye aggregation is believed to be the main cause jeopardizing electron injection (see below). In spite of weak emission of the dyes in the solution (lifetime = 0.13 ns), no discernible emission can be detected for the film state or on TiO_2,

Table 2. DSSC performance parameters of the dyes with and without CDCA.

Dye	J_{SC} [mA cm^2]	V_{OC} [V]	FF	η [%][b]	Dye loading [mol cm^2]
IDT1	4.67 ± 0.05	0.57 ± 0.01	0.74 ± 0.01	1.98 ± 0.02	2.03×10^{-7}
IDT1 + CDCA[a]	0.72 ± 0.01	0.63 ± 0.01	0.74 ± 0.01	0.34 ± 0.00	1.61×10^{-8}
IDT2	3.86 ± 0.05	0.52 ± 0.01	0.69 ± 0.01	1.38 ± 0.01	4.39×10^{-7}
IDT2 + CDCA[a]	1.43 ± 0.16	0.60 ± 0.04	0.78 ± 0.05	0.66 ± 0.07	2.73×10^{-8}
IDT3	7.25 ± 0.26	0.56 ± 0.01	0.67 ± 0.01	2.70 ± 0.10	4.31×10^{-7}
IDT3 + CDCA[a]	10.71 ± 0.12	0.61 ± 0.00	0.69 ± 0.00	4.51 ± 0.05	5.25×10^{-8}
IDT4	6.34 ± 0.34	0.51 ± 0.01	0.60 ± 0.00	1.96 ± 0.08	3.08×10^{-7}
IDT4 + CDCA[a]	12.31 ± 0.48	0.60 ± 0.00	0.64 ± 0.01	4.73 ± 0.11	9.36×10^{-8}
IDT5	7.48 ± 0.18	0.57 ± 0.01	0.60 ± 0.03	2.54 ± 0.08	2.99×10^{-7}
IDT5 + CDCA[a]	13.71 ± 0.72	0.60 ± 0.00	0.61 ± 0.03	5.06 ± 0.05	4.80×10^{-8}
N719	15.88	0.739	0.64	7.48	

[a] 30 mM CDCA was added as the co-adsorbent. [b] The results are given as the mean ± the standard deviations based on three measurements.

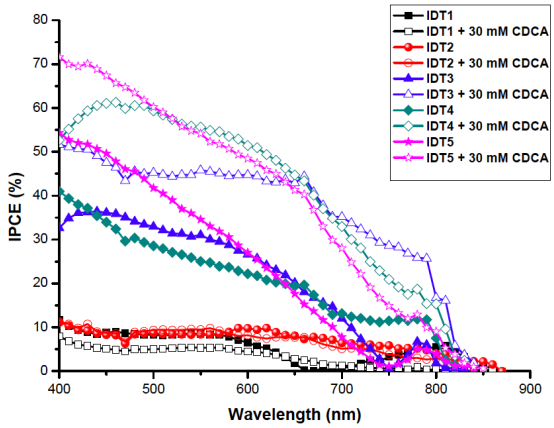

Figure 6. IPCE spectra of DSSCs based on the dyes with 30 mM co-adsorbent CDCA.

which supports the aggregation-induced quenching of the excited states. The low photocurrent (and hence low efficiency) of the IDT-based dye reported by Roncali[17] may indicate a similar problem with dye aggregation. Negative charge trapped at the phenyl ring of the IDT entity, evident from the Mulliken charge difference between the S_0 and S_1 (or S_2) states (see below), may also hamper electron injection. The power conversion efficiencies are in the order **IDT3** (2.70%) > **IDT5** (2.54%) > **IDT1** (1.98%) > **IDT4** (1.96%) > **IDT2** (1.38%). Dyes **IDT3**–**IDT5** have significantly higher J_{SC} values compared with **IDT1** and **IDT2** throughout the whole spectral range. The dye loading amount is shown in Table 2. Dye **IDT1** has the lowest dye loading despite its smallest molecular size. Dye **IDT1** also has a shorter skeleton than the others, and therefore the smaller number of chemical bonds available for rotation may hamper the adsorbed dye molecules in adjusting their relative orientation for more compact packing. The low dye loading of **IDT1** is consistent with its low photocurrent. However, dye loading is not the decisive factor for the cell performance because **IDT2** has the highest loading of all the dyes. Although the inferior light harvesting of **IDT1** and **IDT2** compared with the other dyes certainly is not completely unrelated to their lower J_{SC} values, we speculate that the dye adsorption angles for the latter at the TiO_2 surface do not favor electron injection. In comparison, **IDT2** and **IDT4** have smaller V_{OC} values than the other three. Consequently, **IDT2** has the lowest conversion efficiency overall.

To clarify the origin of the different cell performances among the dyes, we used electrochemical impedance spectroscopy (EIS) and intensity modulated photovoltage spectroscopic (IMVS)[20] measurements to probe the charge recombination (dark current), and the charge extraction method[21] to probe the conduction band edge shift of the TiO_2 after dye adsorption. The correlation plot of V_{OC} and charge density (Q) based on charge extraction method is shown in Figure 7. The

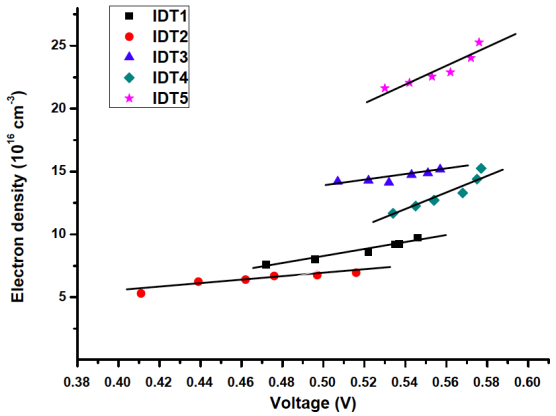

Figure 7. Electron lifetime as a function of V_{OC} based on IMVS measurements.

charges extracted at the same applied voltage decrease in the order **IDT5** > **IDT3** > **IDT4** > **IDT1** > **IDT2**, which should be the order of an upward shift of the TiO_2 conduction band edge. The second circle of the Nyquist plots from the EIS in the dark provides information about charge recombination (dark current), and a larger semicircle means a smaller dark current (Figure 8). The order of decreasing recombination resistance, **IDT5** > **IDT3** > **IDT1** > **IDT4** > **IDT2**, is approximately the same

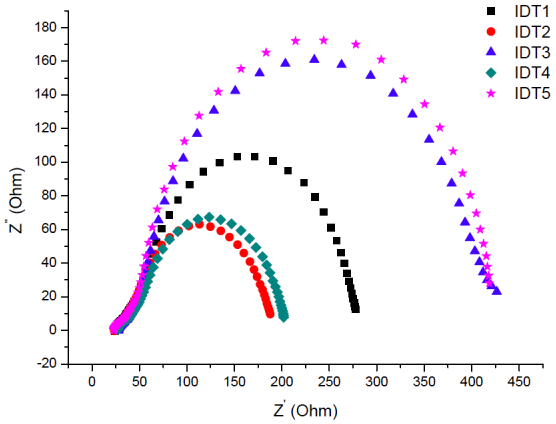

Figure 8. Nyquist plots of DSSCs.

as that of the decreasing V_{OC}. This clearly indicates that charge recombination (dark current) dominates over the conduction band edge shift in shifting the Fermi level of TiO_2. Although **IDT5** does not have the highest dye loading, it is the most efficient for dark current suppression. It is believed that the branched amine donors can more effectively block the close contact of the electrolyte with the TiO_2 surface, similar to 2,3-disubstituted thiophene-based metal-free dyes reported by us.[22] The two alkoxy chains in **IDT3** are also beneficial for dark current suppression. However, the effect diminishes as the spacer between the anchor and IDT increases, possibly owing to the decreased dye loading (**IDT4**) or increased void space in the dye molecules (**IDT2**). The high V_{OC} of **IDT1** can be largely attributed to the significant upward shift of the conduction band edge of TiO_2 adsorbed with **IDT1**.

As dye aggregation jeopardized electron injection and impaired the cell performance, DSSCs with different concentrations of CDCA (30 mM) as the co-adsorbent were also tested. The performance parameters are shown in Table S1 (in the Supporting Information). The cell has the best performance with 30 mM of CDCA for **IDT3** to **IDT5**. However, the cell performance drops significantly for **IDT1** and **IDT2** upon addition of $\geq$10 mM CDCA. The J_{SC} value decreases with addition of even 1 mM CDCA. The dye loading with CDCA co-adsorbent (30 mM during dye soaking) was found to decrease and the decrement differed among dyes (Table 2). Loss of photocurrent as a result of significantly lower dye loading for **IDT1** and **IDT2** compared with the other dyes clearly cannot compensate for the gain from anti-aggregation of the dyes.[23] In contrast, the V_{OC} value increases by more than 60 mV owing to the alleviation of dye aggregation. The other three dyes have significant improvements in the cell performance upon addition of CDCA: $\eta = 4.51\%$, $J_{SC} = 10.71$ mA cm^2, $V_{OC} = 608$ mV, FF = 0.69 for **IDT3**; $\eta = 4.73\%$, $J_{SC} = 12.31$ mA cm^2, $V_{OC} = 604$ mV, FF = 0.64 for **IDT4**; $\eta = 5.06\%$, $J_{SC} = 13.71$ mA cm^2, $V_{OC} = 604$ mV, FF = 0.61 for **IDT5** (Figure 9). Apparently, the loss in dye loading is well compensated by the alleviation of aggregation-induced quenching of the excited dye molecules. It is also interesting that dye aggregation has a substantial contribution to the photocurrent at the near infrared region up to ~800 nm. The cell efficiency of **IDT5** reaches 68% of the N719 standard device (7.48%).

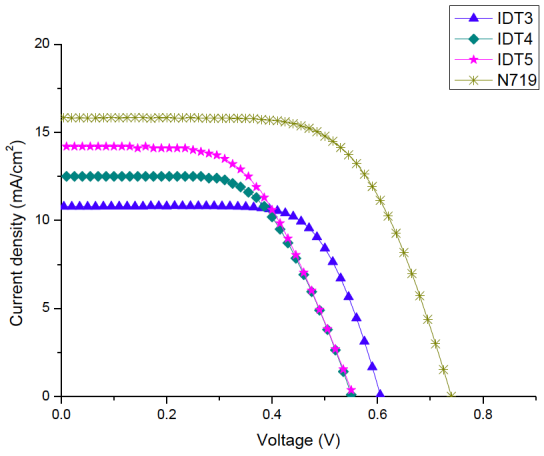

Figure 9. *J–V* curves of DSSCs based on the **IDT1**–**IDT5** dyes with 30 mM of CDCA.

Theoretical Approach

Density functional theory and time-dependent density functional theory (TDDFT) calculations at the B3LYP/6-31G* level by using Q-Chem 4.0 software were carried out. The frontier orbitals and their corresponding energy states are shown in Figure S1 and Figure S2, respectively (in the Supporting Information). The relevant data are shown in Table S2 (in the Supporting Information). The HOMO for the dyes mainly comprises triarylamine and the neighboring spacer, extending to the IDT entity. Except for **IDT5**, the phenyl ring of IDT has only a little contribution to the HOMO. The LUMO comprises the acceptor and the neighboring spacer, extending to the IDT entity. In contrast to the HOMO, there is significant contribution of the phenyl ring of the IDT to the LUMO. The charge-transfer character is evident for the $S_0 \rightarrow S_1$ transition (nearly 100% HOMO$\rightarrow$LUMO). Figure S3 (in the Supporting Information) shows the ground-state geometries of the IDT dyes and the dihedral angles between the two neighboring conjugated segments are indicated. The dihedral angle ($>20^\circ$) between the IDT segment and the arylamine is larger than that ($<14^\circ$) between the IDT and the conjugated thiophene (T) because of the larger steric hindrance in the former. For **IDT5**, both arylamine donors contribute to the electron injection, and the arylamine connected to the phenyl ring of the IDT entity has a smaller contribution owing to the larger dihedral angle between the donor and the IDT entity. However, the large dihedral angle between the donors and the spacer is beneficial for suppressing dye aggregation on the TiO_2 surface. The Mulliken charge shifts for the S_1 and S_2 states (Table S2 in the Supporting Information) were also calculated from the TDDFT results. The charges for the different segments, triarylamine (Tpa), thiophene (T, T1, or T2), IDT, and 2-cyanoacrylic acid, are shown in Figure S4 (in the Supporting Information). Significant negative charge at the IDT entity, especially at the phenyl ring for **IDT1** and **IDT2**, may be partially responsible for the low J_{SC} values of the corresponding cells.

Conclusions

A series of metal-free dyes (**IDT1**–**IDT5**) incorporating an indenothiophene moiety in the conjugated spacer between the triarylamine donor and 2-cyanoacrylic acceptor have been synthesized. These dyes absorb in the visible region up to 700 nm in THF, and even beyond 700 nm when adsorbed onto TiO_2 surfaces as a result of *J*-aggregation. Significant dye aggregation and inefficient electron injection result in the low performances of the fabricated DSSCs. A special feature of these dyes is the non-negligible contribution of photocurrent in the near infrared region. The DSSC based on the dye **IDT5** gives 5.06% efficiency upon addition of CDCA as a co-adsorbent, which is about 68% of the N719-based standard dye.

Experimental Section

Materials and methods

All reactions were performed in oven-dried glassware under a nitrogen atmosphere. Solvents, toluene, *N*,*N*-dimethylformamide (DMF), and tetrahydrofuran (THF) were distilled under a nitrogen atmosphere with sodium, and dichloromethane was distilled from CaH_2. ^{1}H nuclear magnetic resonance (NMR) spectra were obtained with Bruker 300, 400, and 500 MHz spectrometers, and the chemical shifts are reported in parts per million with $CDCl_3$ (7.24 ppm), [D_8]THF (3.58 ppm), or [D_6]DMSO (2.50 ppm) as internal standard. ^{13}C NMR spectra were recorded with a 100 MHz spectrometer with $CDCl_3$ (77.2 ppm), [D_8]THF (67.6 ppm), or [D_6]DMSO (39.5 ppm) as the internal standard.

Assembly and characterization of DSSCs

The 0.4×0.4 cm^2 TiO_2 thin-film photoanode consisted of 12 μm of 20 nm particles as the absorbing layer and 6 μm of 400 nm particles as the scattering layer on fluorine-doped tin oxide (FTO) glass followed by dipping into a THF solution containing 10^{-4} M of the dye sensitizers for 12 h. The electrolyte was composed of 0.5 M lithium iodide (LiI), 0.05 M iodine (I_2), and 0.5 M 4-*tert*-butylpyridine dissolved in acetonitrile. The electrolyte was injected into the seam between the photoanode and Pt counter electrode, which was adhered with a polyimide tape 30 μm in thickness and a square aperture of 0.36 cm^2 was placed on top of the counter electrode. The cell was clipped tightly with a 0.5×0.5 cm^2 cardboard mask on the device. Photoelectrochemical characterizations of the solar cells were measured by an Oriel Class AAA solar simulator (Oriel 94043 A, Newport Corp.). Photocurrent–voltage characteristics of the DSSCs were recorded with a potentiostat/galvanostat (CHI650B, CH Instruments, Inc.) at a light intensity of 100 mW cm^{-1-2} calibrated by an Oriel reference solar cell (Oriel 91150, Newport Corp.). The monochromatic quantum efficiency was detected through a monochromator (Oriel 74100, Newport Corp.) under short-circuit conditions. The intensity of each wavelength was in the range 1–3 mW cm^{-1-2}. Electrochemical impedance spectra (EIS) were carried out under illumination with an open-circuit voltage (V_{OC}) or in the dark at −0.55 V at room temperature. The frequencies explored ranged from 10 mHz to 100 kHz. Intensity-modulated photovoltage spectroscopy (IMVS) was carried out on an electrochemical workstation (Zahner, Zennium) with a frequency response analyzer under an intensity-modulated (10–300 W m^{-2}) white light emitting diode driven by a Zahner (0982wlr02) source supply. The frequency range was set from 100 kHz to 10 mHz.

Quantum chemistry computation

The computations were performed with Q-Chem 4.0 software.[24] Geometry optimization of the molecules was performed by using the hybrid B3LYP and 6-31G* basis set. For each molecule, all conformations were examined and the lowest energy one was used. The same functional was also applied for the calculation of excited states by using time-dependent density functional theory (TDDFT). There exist a number of previous works that employed TDDFT to characterize excited states with charge-transfer character.[25]

(*E*)-Ethyl 2-(2-bromo-8*H*-indeno[2,1-*b*]thiophen-8-ylidene)-2-cyanoacetate (3)

Compound **2** (1.00 g, 3.77 mmol), anhydrous CH_2Cl_2 (30 mL), ethyl cyanoacetate (2.13 g, 18.85 mmol), and *N*-methylmorpholine (3.32 g, 32.80 mmol) were added to an oven-dried Schlenk flask (100 mL) equipped with a stirred bar under a nitrogen atmosphere. $TiCl_4$ (1.57 g, 8.29 mmol) was added and stirred under ultrasonic irradiation conditions for 2 h. Water (20 mL) was added to the crude mixture, which was then extracted with CH_2Cl_2 (20 mL) three times. The combined organic layer was washed with brine, dried over $MgSO_4$, filtered through a filter paper, and concentrated to give the crude mixture. The crude mixture was purified by flash column chromatography (silica gel, 50% CH_2Cl_2/hexanes) to give **3** (0.84 g, 2.33 mmol, 62%) as an orange solid. M.p.: 178–179 °C. ^{1}H NMR (400 MHz, $CDCl_3$): $\delta=8.45$ (d, $J=7.6$ Hz, 1H), 7.31 (t, $J=7.6$ Hz, 1H), 7.21–7.17 (m, 3H), 4.42 (q, $J=7.2$ Hz, 2H), 1.42 ppm (t, $J=7.2$ Hz, 3H). ^{13}C NMR (100 MHz, $CDCl_3$): $\delta=163.9$, 153.3, 153.1, 138.4, 137.9, 135.8, 132.6, 130.2, 128.2, 127.3, 122.6, 120.2, 116.3, 94.6, 63.1, 14.4 ppm. MS-LR-EI: calcd for $C_{16}H_{10}BrNO_2S$ ([*M*]$^+$): 358.9, found: 358.9.

(*E*)-Ethyl-2-cyano-2-(2-(4-(diphenylamino)phenyl)-8*H*-indeno[2,1-*b*]thiophen-8-ylidene)acetate (4)

Compound **3** (0.40 g, 1.11 mmol), *N*,*N*-diphenyl-4-(tributylstannyl)-aniline (0.89 g, 1.67 mmol), $Pd(PPh_3)_4$ (64 mg, 0.05 mmol), PPh_3 (30 mg, 0.11 mmol), and anhydrous toluene (6 mL) were added to an oven-dried Schlenk flask (100 mL) equipped with a stirred bar and heated at 110 °C for 1 d under a nitrogen atmosphere. After removal of the solvent, CH_2Cl_2 (5 mL) and $KF_{(aq)}$ (5 mL) were added. The reaction mixture was added to water (10 mL) and extracted with CH_2Cl_2 (10 mL×3). The combined organic layer was washed with brine, dried over $MgSO_4$, filtered through a filter paper, and concentrated to give the crude mixture. The crude mixture was purified by flash column chromatography (silica gel, 50% CH_2Cl_2/hexanes) to give a red solid **4** (0.29 g, 0.805 mmol, 25%). M.p.: 89–90 °C. ^{1}H NMR (400 MHz, $CDCl_3$): $\delta=8.39$ (d, $J=7.6$ Hz, 1H), 7.53 (d, $J=8.8$ Hz, 2H), 7.31–7.26 (m, 4H), 7.25–7.22 (m, 2H), 7.20 (s, 1H), 7.16–7.12 (m, 5H), 7.08 (t, $J=7.6$ Hz, 2H), 7.03 (d, $J=7.2$ Hz, 2H), 4.39 (q, $J=7.2$ Hz, 2H), 1.41 ppm (t, $J=7.2$ Hz, 3H). ^{13}C NMR (75 MHz, $CDCl_3$): $\delta=164.2$, 160.6, 155.6, 153.3, 149.2, 147.1, 139.9, 138.3, 133.6, 132.1, 129.7, 127.9, 127.1, 126.7, 125.4, 124.1, 122.4, 120.0, 117.1, 114.4, 92.5, 62.6, 14.4 ppm. MS-LR-EI: calcd for $C_{34}H_{24}N_2O_2S$ ([*M*]$^+$): 524.1, found: 524.1.

(*E*)-Ethyl-2-(2-(5-(4-(bis(4-(hexyloxy)phenyl)amino)phenyl)-thiophen-2-yl)-8*H*-indeno[2,1-*b*]thiophen-8-ylidene)-2-cyanoacetate (5)

Compound **3** (0.87 g, 2.42 mmol), 4-(hexyloxy)-*N*-(4-(hexyloxy)phenyl)-*N*-(4-(5-(tributyl-stannyl)thiophen-2-yl)phenyl)aniline (3.95 g, 4.84 mmol), $Pd(PPh_3)_4$ (0.14 g, 0.12 mmol), PPh_3 (63 mg, 0.24 mmol), and anhydrous toluene (12 mL) were added to an oven-dried Schlenk flask (100 mL) equipped with a stirred bar and heated at 110 °C for 1 d under a nitrogen atmosphere. After removal of the solvent, CH_2Cl_2 (10 mL) and $KF_{(aq)}$ (10 mL) were added. The reaction mixture was added to water (20 mL) and extracted with CH_2Cl_2 (20 mL×3). The combined organic layer was washed with brine, dried over $MgSO_4$, filtered through a filter paper, and concentrated to give the crude mixture. The crude mixture was purified by flash column chromatography (silica gel, 70% CH_2Cl_2/hexanes) to give a dark-green solid **5** (1.10 g, 1.36 mmol, 56%). M.p.: 86–87 °C. ^{1}H NMR (400 MHz, $CDCl_3$): $\delta=8.29$ (d, $J=7.6$ Hz, 1H), 7.32 (d, $J=8.8$ Hz, 2H), 7.20 (d, $J=3.6$ Hz, 1H), 7.16 (t, $J=7.6$ Hz, 1H), 7.09–7.04 (m, 6H), 7.01 (d, $J=3.6$ Hz, 1H), 6.92 (s, 1H), 6.87 (d, $J=8.8$ Hz, 2H), 6.83 (d, $J=8.8$ Hz, 4H), 4.31 (q, $J=7.2$ Hz, 2H), 3.93 (t, $J=6.6$ Hz, 4H), 1.81–1.74 (m, 4H), 1.50–1.43 (m, 4H), 1.39–1.32 (m, 8H), 0.91 ppm (t, $J=6.8$ Hz, 6H). ^{13}C NMR (100 MHz, $CDCl_3$): $\delta=$

164.1, 156.0, 155.1, 153.6, 152.7, 149.1, 146.6, 140.2, 139.9, 137.8, 134.4, 133.3, 131.9, 127.9, 127.4, 127.1, 126.8, 126.5, 125.2, 122.7, 120.0, 119.9, 117.0, 115.5, 114.7, 92.2, 68.4, 62.6, 31.8, 29.5, 25.9, 22.8, 14.4, 14.2 ppm. MS-LR-FAB: calcd for $C_{50}H_{50}N_2O_4S_2$ ($[M]^+$): 806.3, found: 806.3.

(*E*)-2-Cyano-2-(2-(4-(diphenylamino)phenyl)-8*H*-indeno[2,1-*b*]thiophen-8-ylidene)acetic acid (IDT1)

$LiOH_{(aq)}$ (2 M, 7.4 mL) was added to a solution of **4** (290 mg, 0.55 mmol) in anhydrous THF (4 mL). After 12 h, the mixture was neutralized with 4 N $HCl_{(aq)}$ and extracted with H_2O (10 mL) and CH_2Cl_2 (10 mL×3). The combined organic layer was dried over $MgSO_4$, filtered through a filter paper, and concentrated to give the crude mixture. The crude mixture was purified by flash column chromatography (silica gel, 10% acetic acid/ethyl acetate) to give a black solid **IDT1** (118 mg, 0.24 mmol, 43%). M.p.: 239–240 °C. ^{1}H NMR (400 MHz, [D$_8$]THF): δ = 8.49 (d, J = 8.0 Hz, 1H), 7.65 (d, J = 7.6 Hz, 2H), 7.54 (s, 1H), 7.42 (d, J = 7.2 Hz, 1H), 7.34 (t, J = 7.2 Hz, 1H), 7.29 (t, J = 8.0 Hz, 4H), 7.22 (td, J = 7.6, 1.2 Hz, 1H), 7.12 (d, J = 8.0 Hz, 4H), 7.06 ppm (t, J = 7.6 Hz, 4H). ^{13}C NMR (125 MHz, [D$_8$]THF): δ = 165.6, 161.0, 156.0, 153.3, 150.2, 148.4, 141.0, 139.5, 134.8, 132.9, 128.7, 128.5, 127.8, 127.2, 126.1, 124.8, 123.6, 120.9, 117.6, 115.5, 94.9 ppm. MS-HR-EI: calcd for $C_{32}H_{20}N_2O_2S$ ($[M]^+$): 496.1245, found: 496.1245. Elemental analysis calcd (%) for $C_{32}H_{20}N_2O_2S$: C 77.40, H 4.06, N 5.64; found: C 77.40, H 4.17, N 5.47.

(*E*)-2-(2-(5-(4-(Bis(4-(hexyloxy)phenyl)amino)phenyl)thiophen-2-yl)-8*H*-indeno[2,1-*b*]thiophen-8-ylidene)-2-cyanoacetic acid (IDT2)

$LiOH_{(aq)}$ (2 M, 6.7 mL) was added to a solution of **5** (400 mg, 0.50 mmol) in anhydrous THF (7 mL). After 12 h, the mixture was neutralized with 4 N $HCl_{(aq)}$ and extracted with H_2O (10 mL) and CH_2Cl_2 (10 mL×3). The combined organic layer was dried over $MgSO_4$, filtered through a filter paper, and concentrated to give the crude mixture. The crude mixture was purified by flash column chromatography (silica gel, 1% acetic acid/ethyl acetate) to give a black solid **IDT2** (94 g, 0.12 mmol, 24%). M.p.: 183–184 °C. ^{1}H NMR (400 MHz, [D$_6$]DMSO): δ = 8.34 (d, J = 8.0 Hz, 1H), 7.62 (s, 1H), 7.57 (d, J = 7.6 Hz, 1H), 7.49 (d, J = 8.8 Hz, 2H), 7.44 (d, J = 4.0 Hz, 1H), 7.40 (t, J = 7.6 Hz, 1H), 7.36 (d, J = 4.0 Hz, 1H), 7.28 (t, J = 7.6 Hz, 1H), 7.04 (d, J = 8.8 Hz, 4H), 6.91 (d, J = 8.8 Hz, 4H), 6.76 (d, J = 8.8 Hz, 2H), 3.93 (t, J = 6.4 Hz, 4H), 1.73–1.66 (m, 4H), 1.43–1.38 (m, 4H), 1.34–1.30 (m, 8H), 0.88 ppm (t, J = 6.8 Hz, 6H). ^{13}C NMR (125 MHz, [D$_6$]DMSO): δ = 206.6, 163.87, 155.52, 151.16, 150.99, 149.45, 148.40, 144.14, 144.07, 139.35, 139.09, 137.17, 134.45, 134.28, 130.95, 126.98, 126.21, 124.45, 124.38, 123.21, 119.96, 118.97, 118.78, 115.71, 115.49, 114.96, 67.61, 30.91, 28.63, 25.12, 21.98, 13.8 ppm. MS-HR-FAB: calcd for $C_{48}H_{46}N_2O_4S_2$ ($[M]^+$): 778.2899, found: 778.2893. Elemental analysis calcd (%) for $C_{48}H_{46}N_2O_4S_2$: C 74.00, H 5.95, N 3.60; found: C 74.21, H 5.83, N 3.62.

2-(5-(4-(Bis(4-(hexyloxy)phenyl)amino)phenyl)thiophen-2-yl)-8*H*-indeno[2,1-*b*]thiophen-8-one (6)

Compound **2** (1.70 g, 6.42 mmol), 4-(hexyloxy)-*N*-(4-(hexyloxy)phenyl)-*N*-(4-(5-(tributylstannyl)thiophen-2-yl)phenyl)aniline (6.29 g, 7.70 mmol), $PdCl_2(PPh_3)_2$ (0.09 g, 0.13 mmol), and anhydrous DMF (13 mL) were added to an oven-dried Schlenk flask (100 mL) equipped with a stirred bar and heated at 80 °C for 14 h under a nitrogen atmosphere. After removal of the solvent, CH_2Cl_2 (10 mL) and $KF_{(aq)}$ (10 mL) were added. The reaction mixture was added to water (20 mL) and extracted with CH_2Cl_2 (20 mL×3). The combined organic layer was washed with brine, dried over $MgSO_4$, filtered through a filter paper, and concentrated to give the crude mixture. The crude mixture was purified by flash column chromatography (silica gel, 50% CH_2Cl_2/hexanes) to give a purple oil **6** (4.45 g, 6.25 mmol, 97%). ^{1}H NMR (400 MHz, $CDCl_3$): δ = 7.42 (d, J = 7.6 Hz, 1H), 7.36 (d, J = 8.8 Hz, 2H), 7.29 (t, J = 7.6 Hz, 1H), 7.23 (d, J = 3.6 Hz, 1H), 7.16–7.11 (m, 3H), 7.08–7.04 (m, 5H), 6.88 (d, J = 8.8 Hz, 2H), 6.83 (d, J = 8.8 Hz, 4H), 3.92 (t, J = 6.4 Hz, 4H), 1.80–1.73 (m, 4H), 1.49–1.42 (m, 4H), 1.35–1.32 (m, 8H), 0.90 ppm (t, J = 7.0 Hz, 6H). ^{13}C NMR (100 MHz, $CDCl_3$): δ = 185.1, 159.3, 156.0, 152.4, 149.1, 146.7, 140.2, 139.4, 138.1, 133.9, 133.5, 133.4, 128.4, 127.1, 126.8, 126.5, 125.1, 123.6, 122.6, 119.9, 119.7, 115.6, 68.4, 31.8, 29.5, 25.9, 22.8, 14.2 ppm. MS-LR-FAB: calcd for $C_{45}H_{45}NO_3S_2$ ($[M]^+$): 711.3, found: 711.3.

4-(5-(8*H*-Indeno[2,1-*b*]thiophen-2-yl)thiophen-2-yl)-*N*,*N*-bis(4-(hexyloxy)phenyl)aniline (7)

Compound **6** (3.26 g, 4.57 mmol) was added to a solution of $AlCl_3$ (1.88 g, 14.10 mmol), BH_3tBuNH_2 (2.57 g, 29.6 mmol) in anhydrous CH_2Cl_2 (30 mL) at 0 °C. After 4 h, the mixture was extracted with H_2O (30 mL) and CH_2Cl_2 (30 mL×3). The combined organic layer was dried over $MgSO_4$, filtered through a filter paper, and concentrated to give the crude mixture. The crude mixture was purified by flash column chromatography (silica gel, 20% CH_2Cl_2/hexanes) to give a yellow oil **7** (1.85 g, 2.65 mmol, 58%). ^{1}H NMR (400 MHz, $CDCl_3$): δ = 7.52 (d, J = 7.6 Hz, 1H), 7.47 (d, J = 7.2 Hz, 1H), 7.40 (d, J = 8.8 Hz, 2H), 7.34–7.31 (m, 2H), 7.20 (t, J = 7.2 Hz, 1H), 7.12 (d, J = 3.6 Hz, 1H), 7.08–7.06 (m, 5H), 6.93 (d, J = 8.8 Hz, 2H), 6.84 (d, J = 8.8 Hz, 4H), 3.94 (t, J = 6.4 Hz, 4H), 3.83 (s, 2H), 1.82–1.75 (m, 4H), 1.51–1.44 (m, 4H), 1.38–1.34 (m, 8H), 0.93 ppm (t, J = 6.8 Hz, 6H). ^{13}C NMR (100 MHz, $CDCl_3$): δ = 155.8, 148.6, 147.9, 146.3, 143.5, 142.7, 141.4, 140.6, 139.3, 136.1, 127.0, 126.9, 126.4, 126.1, 124.9, 124.8, 124.4, 122.3, 120.5, 119.4, 115.5, 114.7, 68.4, 35.1, 31.8, 29.5, 26.0, 22.8, 14.3 ppm. MS-LR-FAB: calcd for $C_{45}H_{47}NO_2S_2$ ($[M]^+$): 697.3, found: 697.3.

(*E*)-5-((2-(5-(4-(Bis(4-(hexyloxy)phenyl)amino)phenyl)thiophen-2-yl)-8*H*-indeno[2,1-*b*]thiophen-8-ylidene)methyl)thiophene-2-carbaldehyde (8)

Compound **7** (1.67 g, 2.39 mmol) and KO*t*Bu (0.30 g, 2.63 mmol) in anhydrous THF (10 mL) and MeOH (5 mL) were added to an oven-dried Schlenk flask under a nitrogen atmosphere. Thiophene-2,5-dicarbaldehyde (0.37 g, 2.63 mmol) in anhydrous THF (10 mL) was added and stirred under ultrasonic irradiation conditions for 3 h. The crude mixture was added to water (20 mL), and then extracted with CH_2Cl_2 (20 mL) three times. The combined organic layer was washed with brine, dried over $MgSO_4$, filtered through a filter paper, and concentrated to give the crude mixture. The crude mixture was purified by flash column chromatography (silica gel, 50% CH_2Cl_2/hexanes) to give **8** as a brown oil (0.82 g, 1.00 mmol, 42%). ^{1}H NMR (400 MHz, $CDCl_3$): δ = 9.85 (s, 1H), 7.65 (d, J = 3.6 Hz, 1H), 7.47 (d, J = 7.6 Hz, 1H), 7.39 (d, J = 3.6 Hz, 1H), 7.35 (d, J = 8.4 Hz, 2H), 7.27 (t, J = 7.2 Hz, 1H), 7.22–7.17 (m, 2H), 7.13–7.11 (m, 3H), 7.07–7.02 (m, 5H), 6.90 (d, J = 8.8 Hz, 2H), 6.83 (d, J = 8.8 Hz, 4H), 3.93 (t, J = 6.4 Hz, 4H), 1.81–1.74 (m, 4H), 1.48–1.45 (m, 4H), 1.37–1.35 (m, 8H), 0.92 ppm (t, J = 6.4 Hz, 6H). ^{13}C NMR (100 MHz, $CDCl_3$): δ = 182.6, 155.9, 151.4, 149.1, 148.8, 144.8, 144.0, 143.9, 142.5, 140.4, 136.6, 136.2, 135.0, 133.8, 133.2, 130.2, 128.6, 127.0, 126.4, 125.7, 125.7, 125.5, 122.5, 120.3, 119.4, 115.5, 114.8, 114.5, 68.4, 31.8, 29.5, 26.0, 22.8, 14.2 ppm. MS-LR-FAB: calcd for $C_{51}H_{49}NO_3S_3$ ($[M]^+$): 819.3, found: 819.3.

(*E*)-5′-((2-(5-(4-(Bis(4-(hexyloxy)phenyl)amino)phenyl)thiophen-2-yl)-8*H*-indeno[2,1-*b*]thiophen-8-ylidene)methyl)-[2,2′-bithiophene]-5-carbaldehyde (9)

Compound **7** (0.60 g, 0.86 mmol) and KO*t*Bu (0.11 g, 0.95 mmol) in anhydrous THF (5 mL) and MeOH (2 mL) were added to an oven-dried Schlenk flask under a nitrogen atmosphere. 2,2′-Bithiophene-5,5′-dicarbaldehyde (0.21 g, 0.95 mmol) in anhydrous THF (5 mL) was added and stirred under ultrasonic irradiation conditions for 3 h. The crude mixture was added to water (7 mL), and then extracted with CH_2Cl_2 (7 mL) three times. The combined organic layer was washed with brine, dried over $MgSO_4$, filtered through a filter paper, and concentrated to give the crude mixture. The crude mixture was purified by flash column chromatography (silica gel, 75% CH_2Cl_2/hexanes) to give **9** as a brown oil (0.10 g, 0.11 mmol, 13%). ^{1}H NMR (400 MHz, $CDCl_3$): δ = 9.79 (s, 1H), 7.57 (d, J = 4.0 Hz, 1H), 7.50 (d, J = 7.6 Hz, 1H), 7.36 (d, J = 8.8 Hz, 2H), 7.33 (d, J = 7.2 Hz, 1H), 7.30 (d, J = 4.0 Hz, 1H), 7.26 (t, J = 4.0 Hz, 1H), 7.21 (t, J = 3.6 Hz, 2H), 7.18 (d, J = 4.4 Hz, 2H), 7.15–7.12 (m, 2H), 7.07–7.04 (m, 5H), 6.90 (d, J = 8.8 Hz, 2H), 6.84 (d, J = 8.8 Hz, 4H), 3.94 (t, J = 6.4 Hz, 4H), 1.82–1.75 (m, 4H), 1.51–1.44 (m, 4H), 1.37–1.33 (m, 8H), 0.93 ppm (t, J = 7.0 Hz, 6H). ^{13}C NMR (100 MHz, $CDCl_3$): δ = 182.5, 155.9, 150.4, 148.8, 146.6, 144.5, 142.9, 142.7, 142.1, 141.7, 140.5, 137.9, 137.4, 135.9, 135.4, 133.7, 131.2, 131.1, 128.0, 127.0, 126.9, 126.4, 125.8, 125.4, 125.2, 124.8, 122.5, 120.3, 119.9, 119.3, 115.6, 115.4, 114.9, 68.5, 31.8, 29.5, 26.0, 22.8, 14.2 ppm. MS-LR-FAB: calcd for $C_{55}H_{51}NO_3S_4$ ($[M]^+$): 901.3, found: 901.3.

(*E*)-3-(5-((*E*)-(2-(5-(4-(Bis(4-(hexyloxy)phenyl)amino)phenyl)-thiophen-2-yl)-8*H*-indeno[2,1-*b*]thiophen-8-ylidene)methyl)thiophen-2-yl)-2-cyanoacrylic acid (IDT3)

A solution of compound **8** (330 mg, 0.40 mmol), cyanoacetic acid (68.5 mg, 0.80 mmol), and ammonium acetate (31.0 mg, 0.40 mmol) in acetic acid (5 mL) was stirred at 105 °C under a nitrogen atmosphere for 12 h. The crude mixture was filtered through a glass filter, and washed with acetic acid to give **IDT3** (290 mg, 0.33 mmol, 82%) as a black solid. M.p.: 247–248 °C. ^{1}H NMR (500 MHz, [D$_8$]THF): δ = 8.44 (s, 1H), 7.92 (d, J = 4.0 Hz, 1H), 7.80 (d, J = 7.5 Hz, 1H), 7.74 (s, 1H), 7.68 (d, J = 4.0 Hz, 1H), 7.53–7.50 (m, 2H), 7.44 (d, J = 8.0 Hz, 2H), 7.41 (d, J = 3.5 Hz, 1H), 7.28–7.18 (m, 3H), 7.04 (d, J = 8.5 Hz, 4H), 6.89–6.84 (m, 6H), 3.94 (t, J = 6.5 Hz, 4H), 1.78–1.73 (m, 4H), 1.51–1.46 (m, 4H), 1.38–1.35 (m, 8H), 0.92 ppm (t, J = 6.5 Hz, 6H). ^{13}C NMR (125 MHz, [D$_8$]THF): δ = 164.2, 157.17, 157.16, 152.6, 149.9, 149.5, 146.0, 145.7, 145.4, 144.0, 141.4, 139.0, 138.7, 137.2, 136.0, 134.3, 134.2, 132.1, 129.3, 127.8, 127.1, 126.83, 126.78, 126.6, 123.7, 121.4, 121.0, 120.3, 116.9, 116.2, 115.8, 101.4, 68.9, 32.7, 30.5, 26.9, 23.7, 14.5 ppm. MS-HR-FAB: calcd for $C_{36}H_{31}N_3O_4S_3$ ($[M]^+$): 886.2933, found: 886.2933. Elemental analysis calcd (%) for $C_{54}H_50N_2O_4S_3$: C 73.11, H 5.68, N 3.16; found: C 73.14, H 5.60, N 3.21.

((*E*)-3-(5-((*E*)-(2-(5-(4-(Bis(4-(hexyloxy)phenyl)amino)phenyl)thiophen-2-yl)-8*H*-indeno[2,1-*b*]thiophen-8-ylidene)methyl)thiophen-2-yl)-2-cyanoacrylic acid (IDT4)

A solution of compound **9** (100 mg, 0.11 mmol), cyanoacetic acid (19 mg, 0.22 mmol), and ammonium acetate (9 mg, 0.11 mmol) in acetic acid (2 mL) was stirred at 105 °C under a nitrogen atmosphere for 12 h. The crude mixture was filtered through a glass filter, and washed with acetic acid to give **IDT4** (80 mg, 0.08 mmol, 75%) as a black solid. M.p.: 261–262 °C. ^{1}H NMR (400 MHz, [D$_8$]THF): δ = 8.37 (s, 1H), 7.86 (d, J = 4.0 Hz, 1H), 7.78 (d, J = 7.2 Hz, 1H), 7.65 (d, J = 7.2 Hz, 3H), 7.55–7.51 (m, 3H), 7.45 (d, J = 8.4 Hz, 2H), 7.35 (d, J = 3.2 Hz, 1H), 7.28–7.23 (m, 2H), 7.20 (t, J = 7.6 Hz, 1H), 7.04 (d, J = 8.4 Hz, 4H), 6.89 (d, J = 8.4 Hz, 2H), 6.85 (d, J = 8.4 Hz, 4H), 3.95 (t, J = 6.4 Hz, 4H), 1.80–1.77 (m, 4H), 1.51–1.46 (m, 4H), 1.38–1.35 (m, 8H), 0.93 ppm (t, J = 6.8 Hz, 6H). ^{13}C NMR (125 MHz, [D$_8$]THF): δ = 164.1, 157.2, 151.7, 149.9, 146.7, 146.4, 145.5, 143.91, 143.86, 142.7, 141.4, 140.2, 139.0, 137.0, 136.6, 136.1, 134.4, 133.0, 132.1, 128.8, 128.2, 127.8, 127.1, 126.8, 126.4, 126.3, 126.2, 123.3, 121.1, 120.2, 116.9, 116.8, 116.22, 116.17, 116.0, 100.4, 68.9, 32.8, 30.5, 26.9, 23.7, 14.6 ppm. MS-HR-FAB: calcd for $C_{58}H_{52}N_2O_4S_4$ ($[M]^+$): 968.2810, found: 968.2784. Elemental analysis calcd (%) for $C_{58}H_{52}N_2O_4S_4$: C 71.87, H 5.41, N 2.89; found: C 71.89, H 5.42, N 2.99.

2,6-Dibromo-8*H*-indeno[2,1-*b*]thiophen-8-one (11)

Br_2 (0.82 g, 5.15 mmol) was added dropwise to a solution of 6-bromo-8*H*-indeno[2,1-*b*]thiophen-8-one (**10**) (0.99 g, 3.73 mmol) and $NaHCO_3$ (0.33 g, 3.73 mmol) in $CHCl_3$ (30 mL) at 0 °C under a nitrogen atmosphere. After 12 h, the mixture was quenched with saturated $Na_2S_2O_{3(aq)}$ and extracted with H_2O (30 mL) and CH_2Cl_2 (30 mL × 3). The combined organic layer was dried over $MgSO_4$, filtered through a filter paper, and concentrated to give the crude mixture. The crude mixture was purified by flash column chromatography (silica gel, 20% CH_2Cl_2/hexanes) to give **11** (0.82 g, 2.38 mmol, 64%). ^{1}H NMR (400 MHz, $CDCl_3$): δ = 7.55 (d, J = 1.6 Hz, 1H), 7.45 (dd, J = 7.8, 1.6 Hz, 1H), 7.14 (s, 1H), 6.98 ppm (d, J = 7.8 Hz, 1H). ^{13}C NMR (100 MHz, $CDCl_3$): δ = 183.2, 157.2, 138.2, 137.8, 136.6, 136.2, 129.2, 127.9, 123.7, 122.8, 121.1 ppm. MS-LR-EI: calcd for $C_{34}H_{24}N_2O_2S$ ($[M]^+$): 341.8, found: 341.8.

2,6-Bis(4-(diphenylamino)phenyl)-8*H*-indeno[2,1-*b*]thiophen-8-one (12)

Compound **11** (0.57 g, 1.66 mmol), *N*,*N*-diphenyl-4-(tributylstannyl)aniline (2.66 g, 4.97 mmol), $Pd(PPh_3)_4$ (0.19 g, 0.17 mmol), and anhydrous DMF (18 mL) were added to an oven-dried Schlenk flask equipped with a stirred bar and heated at 80 °C for 1 d under a nitrogen atmosphere. After removal of the solvent, CH_2Cl_2 (10 mL) and $KF_{(aq)}$ (10 mL) were added. The reaction mixture was added to water (20 mL) and extracted with CH_2Cl_2 (20 mL × 3). The combined organic layer was washed with brine, dried over $MgSO_4$, filtered through a filter paper, and concentrated to give the crude mixture. The crude mixture was purified by flash column chromatography (silica gel, 50% CH_2Cl_2/hexanes) to give **12** (0.64 g, 0.95 mmol, 57%). ^{1}H NMR (400 MHz, $CDCl_3$): δ = 7.66 (s, 1H), 7.44 (t, J = 8.6 Hz, 5H), 7.31–7.25 (m, 8H), 7.17–7.09 (m, 14H), 7.07–7.03 ppm (m, 4H). ^{13}C NMR (100 MHz, $CDCl_3$): δ = 185.3, 159.8, 159.5, 149.2, 147.8, 147.6, 147.1, 140.9, 138.9, 137.7, 133.8, 133.6, 130.7, 129.6, 129.5, 127.4, 127.0, 126.7, 125.3, 124.8, 124.1, 123.6, 123.3, 122.4, 122.0, 119.9, 114.9 ppm. MS-LR-EI: calcd for $C_{47}H_{32}N_2OS$ ($[M]^+$): 672.2, found: 672.2.

4,4′-(8*H*-Indeno[2,1-*b*]thiophene-2,6-diyl)bis(*N*,*N*-diphenylaniline) (13)

Compound **12** (0.64 g, 0.95 mmol) was added to a solution of $AlCl_3$ (0.39 g, 2.93 mmol) and BH_3*t*$BuNH_2$ (0.53 g, 6.14 mmol) in anhydrous CH_2Cl_2 (6 mL) at 0 °C. After 4 h, the mixture was extracted with H_2O (10 mL) and CH_2Cl_2 (10 mL × 3). The combined organic layer was dried over $MgSO_4$, filtered through a filter paper, and concentrated to give the crude mixture. The crude mixture was purified by flash column chromatography (silica gel, 20% CH_2Cl_2/hexanes) to give a pale yellow solid **13** (0.29 g, 0.44 mmol, 46%). M.p.: 173–174 °C. ^{1}H NMR (400 MHz, $CDCl_3$): δ = 7.69 (s, 1H), 7.55–7.50

(m, 6H), 7.41 (s, 1H), 7.28 (t, $J=7.8$ Hz, 8H), 7.16–7.13 (m, 10H), 7.10 (d, $J=8.4$ Hz, 2H), 7.07–7.02 (m, 4H), 3.90 ppm (s, 2H). ^{13}C NMR (100 MHz, $CDCl_3$): $\delta=148.4$, 148.0, 147.9, 147.73, 147.72, 147.47, 147.46, 147.15, 147.11, 142.8, 138.4, 137.3, 135.7, 129.5, 129.5, 127.9, 126.7, 125.6, 124.7, 124.5, 124.3, 124.0, 123.3, 123.1, 119.4, 113.8, 35.0 ppm. MS-LR-EI: calcd for $C_{47}H_{34}N_2S$ ($[M]^+$): 658.2, found: 658.2.

(*Z*)-5′-((2,6-Bis(4-(diphenylamino)phenyl)-8*H*-indeno[2,1-*b*]thiophen-8-ylidene)methyl)-[2,2′-bithiophene]-5-carbaldehyde (14)

Compound **13** (0.29 g, 0.44 mmol) and KO*t*Bu (0.54 g, 0.49 mmol) in anhydrous THF (4 mL) and MeOH (2 mL) were added to an oven-dried Schlenk flask under a nitrogen atmosphere. Thiophene-2,5-dicarbaldehyde (0.10 g, 0.44 mmol) in anhydrous THF (4 mL) was added and stirred under ultrasonic irradiation conditions for 3 h. The crude mixture was added to water (5 mL), and then extracted with CH_2Cl_2 (5 mL) three times. The combined organic layer was washed with brine, dried over $MgSO_4$, filtered through a filter paper, and concentrated to give the crude mixture. The crude mixture was purified by flash column chromatography (silica gel, 67% CH_2Cl_2/hexanes) to give **14** as a dark-red oil (0.14 g, 0.16 mmol, 37%). ^{1}H NMR (500 MHz, $CDCl_3$): $\delta=9.77$ (s, 1H), 7.69 (s, 1H), 7.55 (d, $J=2.4$ Hz, 1H), 7.47–7.45 (m, 4H), 7.38–7.32 (m, 3H), 7.28–7.26 (m, 3H), 7.23–7.20 (m, 8H), 7.12–7.06 (m, 10H), 7.02–6.97 ppm (m, 7H). ^{13}C NMR (125 MHz, $CDCl_3$): $\delta=182.6$, 150.6, 150.0, 148.1, 147.9, 147.5, 147.3, 146.7, 143.4, 142.2, 141.8, 138.1, 137.9, 137.5, 135.6, 134.9, 134.1, 131.5, 131.3, 129.6, 129.5, 128.4, 127.8, 127.0, 126.9, 126.5, 125.0, 124.8, 124.6, 124.2, 123.6, 123.4, 123.1, 119.5, 118.5, 115.3, 114.3 ppm. MS-LR-FAB: calcd for $C_{57}H_{38}N_2OS_3$ ($[M]^+$): 862.2, found: 862.2.

(*E*)-3-(5′-((*Z*)-(2,6-Bis(4-(diphenylamino)phenyl)-8*H*-indeno[2,1-*b*]thiophen-8-ylidene)methyl)-[2,2′-bithiophen]-5-yl)-2-cyanoacrylic acid (IDT5)

A solution of compound **14** (140 mg, 0.16 mmol), cyanoacetic acid (28 mg, 0.33 mmol), and ammonium acetate (13 mg, 0.16 mmol) in acetic acid (5 mL) was stirred at 105 °C under a nitrogen atmosphere for 12 h. The crude mixture was filtered through a glass filter, and washed with acetic acid to give the crude mixture. The crude mixture was purified by flash column chromatography (silica gel, 2% acetic acid/CH_2Cl_2) to give **IDT5** (120 mg, 0.13 mmol, 82%) as a black solid. M.p.: 268–269 °C. ^{1}H NMR (400 MHz, [D$_8$]THF): $\delta=$ 8.35 (s, 1H), 8.11 (s, 1H), 7.86–7.82 (m, 2H), 7.69–7.64 (m, 5H), 7.62 (d, $J=3.6$ Hz, 1H), 7.55–7.53 (m, 3H), 7.30–7.24 (m, 8H), 7.15–6.99 ppm (m, 17H). ^{13}C NMR (100 MHz, [D$_8$]THF): $\delta=151.73$, 150.82, 149.12, 149.10, 149.00, 148.71, 148.62, 148.26, 146.10, 145.72, 144.71, 142.70, 139.72, 139.03, 139.01, 136.82, 135.88, 134.84, 133.18, 132.15, 130.37, 130.24, 129.66, 128.64, 128.11, 127.66, 127.64, 126.97, 126.25, 125.72, 125.42, 125.23, 124.41, 124.36, 123.85, 120.30, 119.65, 117.13, 116.97, 115.42 ppm. MS-HR-FAB: calcd for $C_{60}H_{39}N_3O_2S_3$ ($[M]^+$): 929.2204, found: 929.2197. Elemental analysis calcd (%) for $C_{60}H_{39}N_3O_2S_3$: C 77.47, H 4.23, N 4.52; found: C 77.47, H 4.37, N 4.52.

Acknowledgments

This work was supported by the Academia Sinica (AC) and the Ministry of Science and Technology (Taiwan). We also thank the Instrumental Center of the Institute of Chemistry, Academia Sinica for support.

Keywords: aggregation · dye-sensitized solar cells · heterocycles · indeno[2,1-*b*]thiophene · sensitizers

[1] B. O'Regan, M. Grätzel, *Nature* **1991**, *353*, 737–740.
[2] a) Y. K. Eom, I. T. Choi, S. H. Kang, J. Lee, J. Kim, M. J. Ju, H. K. Kim, *Adv. Energy Mater.* **2015**, *5*, 1500300; b) C.-Y. Chen, M. Wang, J.-Y. Li, N. Pootrakulchote, L. Alibabaei, C.-H. Ngoc-le, J.-D. Decoppet, J.-H. Tsai, C. Grätzel, C.-G. Wu, S. M. Zakeeruddin, M. Grätzel, *ACS Nano* **2009**, *3*, 3103–3109; c) H. Ozawa, Y. Yamamoto, H. Kawaguchi, R. Shimizu, H. Arakawa, *ACS Appl. Mater. Interfaces* **2015**, *7*, 3152–3161; d) G. C. Vougioukalakis, A. I. Philippopoulos, T. Stergiopoulos, P. Falaras, *Coord. Chem. Rev.* **2011**, *255*, 2602–2621; e) F. Gao, Y. Wang, D. Shi, J. Zhang, M. Wang, X. Jing, R. Humphry-Baker, P. Wang, S. M. Zakeeruddin, M. Grätzel, *J. Am. Chem. Soc.* **2008**, *130*, 10720–10728.
[3] a) S. Mathew, A. Yella, P. Gao, R. Humphry-Baker, F. E. CurchodBasile, N. Ashari-Astani, I. Tavernelli, U. Rothlisberger, M. K. Nazeeruddin, M. Grätzel, *Nat. Chem.* **2014**, *6*, 242–247; b) Y. Xie, Y. Tang, W. Wu, Y. Wang, J. Liu, X. Li, H. Tian, W.-H. Zhu, *J. Am. Chem. Soc.* **2015**, *137*, 14055–14058; c) H. Jia, X. Ju, M. Zhang, Z. Ju, H. Zheng, *Phys. Chem. Chem. Phys.* **2015**, *17*, 16334–16340; d) M. Urbani, M. Grätzel, M. K. Nazeeruddin, T. Torres, *Chem. Rev.* **2014**, *114*, 12330–12396.
[4] a) C.-P. Lee, R. Y.-Y. Lin, L.-Y. Lin, C.-T. Li, T.-C. Chu, S.-S. Sun, J. T. Lin, K.-C. Ho, *RSC Adv.* **2015**, *5*, 23810–23825; b) L. M. Gonçalves, V. de ZeaBermudez, H. A. Ribeiro, A. M. Mendes, *Energy Environ. Sci.* **2008**, *1*, 655–667; c) A. Mishra, M. K. R. Fischer, P. Bauërle, *Angew. Chem. Int. Ed.* **2009**, *48*, 2474–2499; *Angew. Chem.* **2009**, *121*, 2510–2536; d) Y. Wu, W. Zhu, *Chem. Soc. Rev.* **2013**, *42*, 2039–2058.
[5] Z. Yao, H. Wu, Y. Li, J. Wang, J. Zhang, M. Zhang, Y. Guo, P. Wang, *Energy Environ. Sci.* **2015**, *8*, 3192–3197.
[6] K. Kakiage, Y. Aoyama, T. Yano, K. Oya, J.-i. Fujisawa, M. Hanaya, *Chem. Commun.* **2015**, *51*, 15894–15897.
[7] S. Chaurasia, C.-J. Liang, Y.-S. Yen, J. T. Lin, *J. Mater. Chem. C* **2015**, *3*, 9765–9780.
[8] a) G. Zhou, N. Pschirer, J. C. Schöneboom, F. Eickemeyer, M. Baumgarten, K. Müllen, *Chem. Mater.* **2008**, *20*, 1808–1815; b) S. Chaurasia, Y.-C. Chen, H.-H. Chou, Y.-S. Wen, J. T. Lin, *Tetrahedron* **2012**, *68*, 7755–7762.
[9] N. J. Zhou, K. Prabakaran, B. H. Lee, S. H. Chang, K. Harutyunyan, P. J. Guo, M. R. Butler, A. Timalsina, M. J. Bedzyk, M. A. Ratner, S. Vegiraju, S. Yau, C. G. Wu, R. P. H. Chang, A. Facchetti, M. C. Chen, T. B. Marks, *J. Am. Chem. Soc.* **2015**, *137*, 4414–4423.
[10] a) L. Cai, T. Moehl, S.-J. Moon, J.-D. Decoppet, R. Humphry-Baker, Z. Xue, L. Bin, S. M. Zakeeruddin, M. Gräzel, *Org. Lett.* **2014**, *16*, 106–109; b) J. Kim, Y. Jo, W.-Y. Choi, Y. Jun, C. Yang, *Tetrahedron Lett.* **2011**, *52*, 2764–2766; c) J.-H. Chen, C.-H. Tsai, S.-A. Wang, Y.-Y. Lin, T.-W. Huang, S.-F. Chiu, C.-C. Wu, K.-T. Wong, *J. Org. Chem.* **2011**, *76*, 8977–8985.
[11] a) R. Y.-Y. Lin, H.-W. Lin, Y.-S. Yen, C.-H. Chang, H.-H. Chou, P.-W. Chen, C.-Y. Hsu, Y.-C. Chen, J. T. Lin, K.-C. Ho, *Energy Environ. Sci.* **2013**, *6*, 2477–2486; b) H. Li, Y. Yang, Y. Hou, R. Tang, T. Duan, J. Chen, H. Wang, H. Han, T. Peng, X. Chen, Q. Li, Z. Li, *ACS Sustainable Chem. Eng.* **2014**, *2*, 1776–1784; c) R. Tarsang, V. Promarak, T. Sudyoadsuk, S. Namuangruk, N. Kungwan, P. Khongprachae, S. Jungsuttiwong, *RSC Adv.* **2015**, *5*, 38130–38140.
[12] a) C.-J. Yang, Y. J. Chang, M. Watanabe, Y.-S. Hon, T. J. Chow, *J. Mater. Chem.* **2012**, *22*, 4040–4049; b) H. Tian, X. Yang, R. Chen, Y. Pan, L. Li, A. Hagfeldt, L. Sun, *Chem. Commun.* **2007**, 3741–3743; c) Y. Hua, S. Chang, H. Wang, D. Huang, J. Zhao, T. Chen, W. Y. Wong, W. K. Wong, X. Zhu, *J. Power Sources* **2013**, *243*, 253–259; d) Y. Hua, S. Chang, D. Huang, X. Zhou, X. Zhu, J. Zhao, T. Chen, W.-Y. Wong, W.-K. Wong, *Chem. Mater.* **2013**, *25*, 2146–2153; e) W.-I. Hung, Y.-Y. Liao, T.-H. Lee, Y.-C. Ting, J.-S. Ni, W.-S. Kao, J. T. Lin, T.-C. Wei, Y.-S. Yen, *Chem. Commun.* **2015**, *51*, 2152–2155; f) R. Y.-Y. Lin, F.-L. Wu, C.-T. Li, P.-Y. Chen, K.-C. Ho, J. T. Lin, *ChemSusChem* **2015**, *8*, 2503–2513; g) Z. Iqbal, W.-Q. Wu, Z.-S. Huang, L. Wang, D.-B. Kuang, H. Meier, *Dyes Pigm.* **2016**, *124*, 63–71.
[13] a) Z. Wang, M. Liang, Y. Tan, L. Ouyang, Z. Sun, S. Xue, *J. Mater. Chem. A* **2015**, *3*, 4865–4874; b) P. Dai, L. Yang, M. Liang, H. Dong, P. Wang, C.

Zhang, Z. Sun, S. Xue, *ACS Appl. Mater. Interfaces* **2015**, *7*, 22436 – 22447.
[14] a) Z. S. Huang, X. F. Zang, T. Hua, L. Wang, H. Meier, D. Cao, *ACS Appl. Mater. Interfaces* **2015**, *7*, 20418 – 20429; b) J. S. Ni, W. S. Kao, H. J. Chou, J. T. Lin, *ChemSusChem* **2015**, *8*, 2932 – 2939.
[15] a) Z. Yao, M. Zhang, H. Wu, L. Yang, R. Li, P. Wang, *J. Am. Chem. Soc.* **2015**, *137*, 3799 – 3802; b) Z. Yao, M. Zhang, R. Li, L. Yang, Y. Qiao, P. Wang, *Angew. Chem. Int. Ed.* **2015**, *54*, 5994 – 5998; *Angew. Chem.* **2015**, *127*, 6092 – 6096; c) H. Choi, M. Shin, K. Song, M.-S. Kang, Y. Kang, J. Ko, *J. Mater. Chem. A* **2014**, *2*, 12931 – 12939; d) K. Lim, C. Kim, J. Song, T. Yu, W. Lim, K. Song, P. Wang, N. Zu, J. Ko, *J. Phys. Chem. C* **2011**, *115*, 22640 – 22646; e) S. H. Chou, C. H. Tsai, C. C. Wu, D. Kumar, K. T. Wong, *Chem. Eur. J.* **2014**, *20*, 16574 – 16582; f) K. Lim, M. J. Ju, J. Song, I. T. Choi, K. Do, H. Choi, K. Song, H. K. Kim, J. Ko, *ChemSusChem* **2013**, *6*, 1425 – 1431.
[16] A. Leliège, C. H. L. Régent, M. Allain, P. Blanchard, J. Roncali, *Chem. Commun.* **2012**, *48*, 8907 – 8909.
[17] D. Demeter, F. Melchiorre, P. Biagini, R. Po, J. Roncali, *Tetrahedron Lett.* **2016**, *57*, 505 – 508.
[18] A. Leliège, J. Grolleau, M. Allain, P. Blanchard, D. Demeter, T. Rousseau, J. Roncali, *Chem. Eur. J.* **2013**, *19*, 9948 – 9960.
[19] A. L. Capodilupo, L. De Marco, E. Fabiano, R. Giannuzzi, A. Scrascia, C. Clarlucci, G. A. Corree, M. P. Cipolla, G. Gigli, G. Ciccarella, *J. Mater. Chem. A* **2014**, *2*, 14181 – 14188.
[20] L.-L. Li, Y.-C. Chang, H.-P. Wu, E. W.-G. Diau, *Int. Rev. Phys. Chem.* **2012**, *31*, 420 – 467.
[21] a) M. J. Griffith, K. Sunahara, P. Wagner, K. Wagner, G. G. Wallace, D. L. Officer, A. Furube, R. Katoh, S. Mori, A. J. Mozer, *Chem. Commun.* **2012**, *48*, 4145 – 4162; b) S. B. Mane, J. Y. Hu, Y. C. Chang, L. Luo, E. W.-G. Diau, C. H. Hung, *Chem. Commun.* **2013**, *49*, 6882 – 6884.
[22] K. R. Justin Thomas, Y.-C. Hsu, J. T. Lin, K.-M. Lee, K.-C. Ho, C.-H. Lai, Y.-M. Cheng, P.-T. Chou, *Chem. Mater.* **2008**, *20*, 1830 – 1840.
[23] V. S. Manthou, E. K. Pefkianakis, P. Falaras, G. C. Vougioukalakis, *ChemSusChem* **2015**, *8*, 588 – 599.
[24] Q-CHEM, Version 4.0.1, Y. Shao, L. Fusti-Molnar, Y. Jung, J. Kussmann, C. Ochsenfeld, S. T. Brown, A. T. B. Gilbert, L. V. Slipchenko, S. V. Levchenko, D. P. O'Neill, R. A. DiStasio, Jr., R. C. Lochan, T. Wang, G. J. O. Beran, N. A. Besley, J. M. Herbert, C. Y. Lin, T. Van Voorhis, S. H. Chien, A. Sodt, R. P. Steele, V. A. Rassolov, P. E. Maslen, P. P. Korambath, R. D. Adamson, B. Austin, J. Baker, E. F. C. Byrd, H. Dachsel, R. J. Doerksen, A. Dreuw, B. D. Dunietz, A. D. Dutoi, T. R. Furlani, S. R. Gwaltney, A. Heyden, S. Hirata, C.-P. Hsu, G. Kedziora, R. Z. Khaliullin, P. Klunzinger, A. M. Lee, M. S. Lee, W. Liang, I. Lotan, N. Nair, B. Peters, E. I. Proynov, P. A. Pieniazek, Y. M. Rhee, J. Ritchie, E. Rosta, C. D. Sherrill, A. C. Simmonett, J. E. Subotnik, H. L. Woodcock III, W. Zhang, A. T. Bell, A. K. Chakraborty, D. M. Chipman, F. J. Keil, A. Warshel, W. J. Hehre, H. F. Schaefer III, J. Kong, A. I. Krylov, P. M. W. Gill, M. Head-Gordon, Z. Gan, Y. Zhao, N. E. Schultz, D. Truhlar, E. Epifanovsky, M. Oana, R. Baer, B. R. Brooks, D. Casanova, J.-D. Chai, C.-L. Cheng, C. Cramer, D. Crittenden, A. Ghysels, G. Hawkins, E. G. Hohenstein, C. Kelley, W. Kurlancheek, D. Liotard, E. Livshits, P. Manohar, A. Marenich, D. Neuhauser, R. Olson, M. A. Rohrdanz, K. S. Thanthiriwatte, A. J. W. Thom, V. Vanovschi, C. F. Williams, Q. Wu, Z.-Q. You, A. Aspuru-Guzik, C. Chang, R. G. Edgar, E. Sundstrom, J. Parkhill, K. Lawler, M. Gordon, M. Schmit, N. Shenvi, D. Lambrecht, M. Goldey, R. Olivares-Amaya, Y. Bernard, L. Vogt, M. Watson, J. Liu, S. Yeganeh, B. Kaduk, O. Vydrov, X. Xu, I. Kaliman, K. Khistyaev, N. Russ, I. Y. Zhang, W. A. Goddard III, F. Liu, R. King, A. Landau, M. Wormit, A. Dreuw, M. Diedenhofen, A. Klamt, A. W. Lange, D. Ghosh, D. Kosenkov, T. Kus, A. Landou, D. Zuev, J. Deng, S. P. Mao, Y. C. Su, D. Small, L. D. Jacobson, Q-Chem. Inc., Pittsburgh, PA, **2011**.
[25] a) H. M. Vaswani, C.-P. Hsu, M. Head-Gordon, G. R. Fleming, *J. Phys. Chem. B* **2003**, *107*, 7940 – 7946; b) Y. Kurashige, T. Nakajima, S. Kurashige, K. Hirao, Y. Nishikitani, *J. Phys. Chem. A* **2007**, *111*, 5544 – 5548.

Manuscript received: March 2, 2016
Revised: March 29, 2016
Accepted Article published: April 7, 2016
Final Article published: ■■ ▮▮, 0000

FULL PAPER

Solar Cell Sensitizers

Chia-Jung Liang, Yu-Ju Lin, Yung-Sheng Yen, Jiann T. Lin, Ming-Chang P. Yeh**

■■ – ■■

Metal-Free Indeno[2,1-*b*]thiophene-Based Sensitizers for Dye-Sensitized Solar Cells

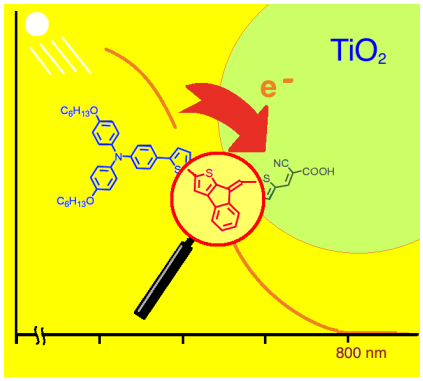

Anchoring thiophenes: A series of indeno[2,1-*b*]thiophene-containing organic dyes (**IDT1**–**IDT5**) has been employed as sensitizers for dye-sensitized solar cells, and the UV/Vis spectra are measured beyond 700 nm. Among them, dyes **IDT3**–**IDT5** with the thiophene unit conjugated with an anchor have better light harvesting and higher J_{SC} values. Furthermore, **IDT5** with chenodeoxycholic acid (CDCA) as the co-adsorbent has the highest power conversion efficiency (5.06%), which is 68% of the standard device based on N719 dye.